Plasmon-assisted photoluminescence enhancement of single-walled carbon nanotubes on metal surfaces

Takerou Sakashita,[1] Yuhei Miyauchi,[1,2] Kazunari Matsuda,[1,a)] and Yoshihiko Kanemitsu[1,3]
[1]*Institute for Chemical Research, Kyoto University, Uji, Kyoto 611-0011, Japan*
[2]*Center for Integrated Science and Engineering, Columbia University, New York, New York 10027, USA*
[3]*Photonics and Electronics Science and Engineering Center, Kyoto University, Kyoto 615-8510, Japan*

(Received 2 May 2010; accepted 2 July 2010; published online 11 August 2010)

We demonstrated photoluminescence (PL) enhancement in single carbon nanotubes using localized surface plasmons. Single nanotube spectroscopy revealed triple the PL intensity enhancement for carbon nanotubes on rough Au surfaces as on fused silica surfaces. The PL enhancement depends on the excitation wavelength and distance between the carbon nanotubes and the Au surface. The degree of PL enhancement is determined by the electric field enhancement from the localized surface plasmon and the energy transfer from the carbon nanotube to the metal surface. © *2010 American Institute of Physics*. [doi:10.1063/1.3467834]

The optical properties of single-walled carbon nanotubes (SWNTs) are of great interest both from a fundamental physics viewpoint and in terms of their potential applications.[1,2] SWNTs have unique optical properties, such as diameter (chirality)-dependent energy gaps and near-infrared photoluminescence (PL),[3] and are among the most promising candidates for nanoscale optoelectronic devices. Exciton dynamics dominate the optical properties in SWNTs because the excited electrons and holes are strongly confined in one-dimensional (1D) materials and form a bound exciton state due to strong Coulomb interactions.[4] Optical devices and applications such as light-emitting diodes,[5] single-photon sources,[6] and fluorescent biolabeling markers[7] have been demonstrated based on luminescence processes arising from exciton recombination in SWNTs. The performance of these optical devices and applications is directly determined from the PL quantum efficiency. Unfortunately, the reported PL quantum efficiencies in SWNTs are typically rather low.[8,9] In addition to improving the quantum efficiency itself, the excitation and recombination rates of the excitons should be enhanced by modifying the external field, thereby improving the performance of the nanotube optical devices and their applications. The excitonic responses in semiconductor nanostructures can be modulated via interactions at the interface between the semiconductor and the metal nanostructures, since the localized surface plasmon creates a strong localized electric field near the metal nanostructure.[10–13] We anticipate that localized surface plasmons will interact strongly with the excitons and will markedly modify the optical properties of SWNTs near metal surfaces.

In this paper, we report the PL properties of a single carbon nanotube on a rough metal surface. Single nanotube spectroscopy revealed triple the PL enhancement for SWNTs on rough Au surfaces. The detailed mechanism of plasmon-assisted PL enhancement is discussed based on the electric field enhancement due to localized surface plasmons and the energy transfer from the SWNT to the metal surface.

The CoMoCAT SWNTs were isolated by dispersion in a solution of toluene with 0.07 wt % poly[9,9-dioctylfluorenyl-2,7-diyl] (PFO) as specified in the procedure developed by Nish *et al.*[14] Single nanotube PL measurements at room temperature were taken under a wide-field luminescence microscope. The SWNTs were excited with linear-polarized laser diode (λ=785, 685, 658, 639, and 532 nm) and Ar^+ lasers (514.5 and 488 nm). The excitation power density on the sample was about 500 W/cm^2. The SWNTs were dispersed directly on fused silica substrates or Au films with rough and flat surfaces[12] using a spin-coating technique. The rough-surface Au substrates were fabricated by an Ar^+ sputtering method and thermally annealed at 600 °C under $\sim 10^{-2}$ Torr atmosphere. The poly(methyl methacrylate) (PMMA) in toluene solutions were spin-coated on the rough-surface Au substrates to control the distance between the SWNTs and Au surfaces. The nominal thickness of the PMMA layer was controlled by its concentration in the toluene. The insets in Figs. 1(c) and 1(d) show topographic images of the flat and rough Au surfaces, with the same vertical scales as obtained by atomic force microscopy. The rough Au surfaces were

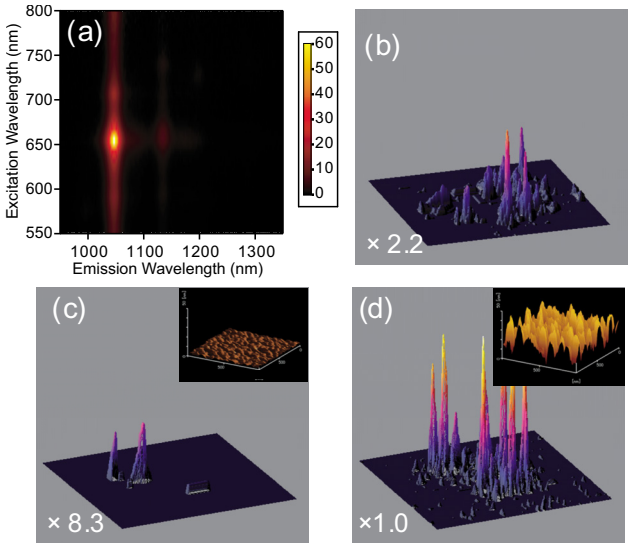

FIG. 1. (Color online) (a) PL excitation map of PFO-dispersed SWNTs in toluene. [(b)–(d)] PL images of single carbon nanotubes on the fused silica, flat Au, and rough Au surfaces, respectively. All image sizes are 40 ×40 μm^2. Inset: Topographic images of rough and flat Au surfaces measured using atomic force microscopy with a vertical scale of ±25 nm and area of 1×1 μm^2.

a)Electronic mail: matsuda@scl.kyoto-u.ac.jp.

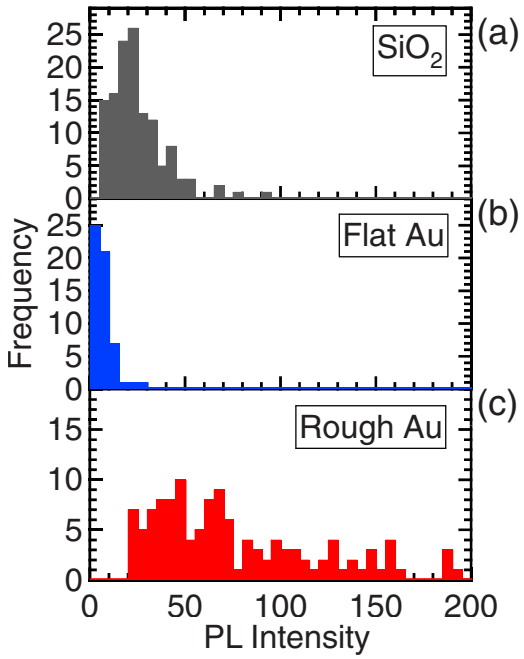

FIG. 2. (Color online) [(a)–(c)] Histograms of the PL intensity of about 100 single carbon nanotubes on fused silica, flat Au, and rough Au surfaces, respectively. The rough Au substrate has a PMMA layer of 15 nm.

composed of particles with height differences of a root mean square (rms) value of 7 nm, and with lateral sizes ranging from 60 to 120 nm. In contrast, the topographic rms value for the flat Au surfaces was estimated at only about 0.5 nm.

Figure 1(a) shows the PL excitation map of PFO-dispersed SWNTs. The distinct PL excitation peak shows that most of the SWNTs, including those in the PFO-dispersed samples, have a (7,5) chiral index.[15] Figures 1(b)–1(d) show PL images of (7,5) single carbon nanotubes on the fused silica, flat Au, and rough Au surfaces, respectively, obtained with an excitation wavelength of 658 nm. We used the rough Au substrate with a PMMA layer of 15 nm. The multiplication of the vertical axes of each image is indicated in the figure. Each peak for all the images comes from the PL signal from a single carbon nanotube. This significant PL intensity enhancement of the single carbon nanotubes on rough Au surfaces can be compared to the PL intensity on fused silica, while the PL intensity on the flat Au surface is even weaker than that on the fused silica. This experimental result indicates that the PL enhancement strongly depends on the metal's surface roughness.

We measured the PL intensities of about 100 single carbon nanotubes on each surface to quantitatively evaluate the PL intensity enhancement. Figures 2(a)–2(c) show histograms of the PL intensity of single carbon nanotubes on fused silica, flat Au, and rough Au surfaces, respectively. The PL intensities on the fused silica are distributed because the carbon nanotubes align randomly on the substrate and the absorption probability strongly depends on the relative angle between the light polarization and the nanotube direction on the substrate. Furthermore, the length variation of the carbon nanotubes in the sonication processed samples[16] also contributes to a distribution in the PL intensities. The averaged PL intensity of the single carbon nanotubes on the rough Au surface, I_{metal}, is observed to be about three times higher than that on the fused silica I_0; i.e., the averaged enhancement factor, I_{metal}/I_0, is estimated to be ~3. Note that the maximum reached PL intensity enhancement for the nanotube on the rough Au surface is ~10. Conversely, the PL enhancement is not observed in the histograms for the flat Au surface.

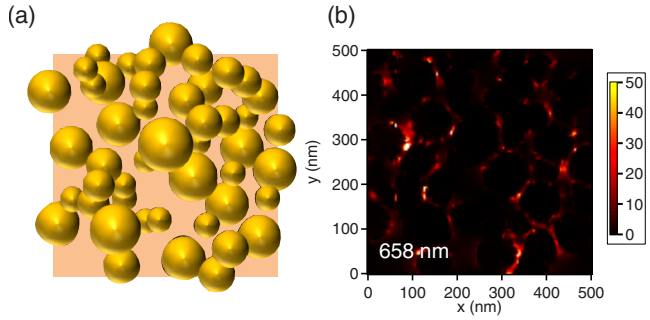

FIG. 3. (Color online) (a) Numerical simulation models of the local electric field on the rough Au surface. (b) Calculated electric field distributions on the rough Au surface. The incident light (λ=658 nm) is *x*-polarized with a value of unity in air.

The electric field distributions on the rough metal surfaces were simulated by the three-dimensional (3D) finite-difference time-domain (FDTD) method to explain the experimentally observed PL enhancement. Figure 3(a) shows the 3D model of the rough Au surface, derived from the topographic images in the inset of Fig. 1(d), used for the FDTD simulations. The complex Au dielectric constants were approximated using the Drude and Lorentzian model, and *x*-polarized plane-wave illumination (λ=658 nm) was used. Figure 3(b) shows the simulated electric field intensity $|E/E_0|^2$ distributions at the z=15 nm plane on the rough Au surface; the intensities of the electric field are normalized by those on the fused silica surface $|E_0|^2$. The electric field intensity is concentrated, and typically 20-fold enhanced, at the edges of the metal structures in parallel with the polarization direction due to the localized surface plasmon resonance. The electric field distributions are spatially inhomogeneous with the maximum field intensity reached being 50 times higher in the small gap between the metal structures.

Figure 4(a) shows the absorption spectrum of the rough Au substrate with a PMMA layer. The absorption peak at around 600 nm comes from the localized surface plasmon resonance of the Au nanostructures. Note that the PL wavelength of (7,5) SWNTs is away from the localized surface plasmon resonances. In the PL process, both the excitation and emission processes contribute to the PL enhancement, with the absorption spectrum indicating that the excitation process plays an important role in the experimentally observed PL enhancement on the rough Au surfaces.

We measured the SWNT PL enhancement on the rough Au surface, I_{metal}/I_0, with varying excitation wavelengths and plotted the results in Fig. 4(a). The PL enhancement depends on the excitation wavelength and the results show the maximum value around 600–700 nm. This experimental result is almost the same as the absorption peak due to the surface plasmon resonance.

We also measured the PL intensity enhancement on the rough Au substrate with a PMMA layer by varying the distance between the carbon nanotubes and the Au surface. The nominal distance between the two is controlled by changing the thickness of the PMMA layer. Figure 4(b) shows the PL intensity enhancement dependence on the distance between the SWNTs and the rough Au surface, obtained by the exci-

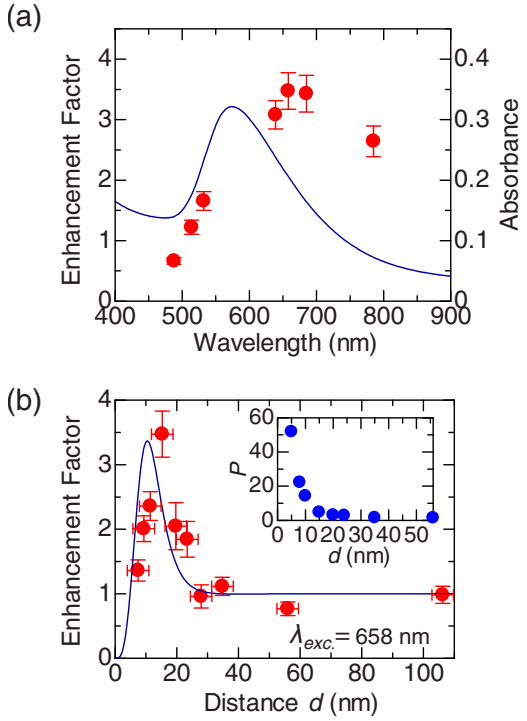

FIG. 4. (Color online) (a) Absorption spectrum of rough Au substrate with a PMMA layer (solid line) and excitation wavelength dependence of the SWNT PL intensity enhancement I_{metal}/I_0 on the rough Au surface with an optimized PMMA layer of 15 nm (solid circles). (b) Distance dependence of the PL intensity enhancement factor I_{metal}/I_0, obtained by the excitation wavelength of 658 nm. The solid line shows the calculated result using Eq. (1). Inset shows the distance dependence of $P(\lambda_{exc.},d)$ from the FDTD simulation.

tation wavelength of 658 nm. The enhancement shows a maximum value of about 15 nm, which indicates the contribution of competing processes.

The metal surfaces play both the role of a strong localized electric field generator and energy dissipation sink.[17,18] Hence, the PL of carbon nanotubes on metal surfaces is totally determined by two competing processes: shortening of the excited state lifetime by the energy transfer to the metal surface and enhancement of the absorption rate due to the localized surface plasmon.[17,18] The PL enhancement factor, defined as a function of distance d and wavelength of the excitation laser light $\lambda_{exc.}$, can be approximately described as follows:

$$\frac{I_{metal}}{I_0} = P(\lambda_{exc.},d)\frac{\gamma_{rad}+\gamma_{nonrad}}{\gamma_{rad}+\gamma_{nonrad}+\gamma_{nonmetal}(d)}, \quad (1)$$

where γ_{rad} and γ_{nonrad} are the radiative and nonradiative decay rates of the excitons, respectively, $\gamma_{nonmetal}$ is the exciton energy transfer rate from the SWNTs to the metal surface, and $P(\lambda_{exc.},d)=|E(\lambda_{exc.},d)/E_0|^2$ is the electric field intensity enhancement due to the localized surface plasmon resonance. The distance dependence of $P(\lambda_{exc.},d)$ is calculated from the FDTD simulation, as shown in inset of Fig. 4(b). Furthermore, the $\gamma_{nonmetal}$ is assumed to be the surface transfer rate $(\propto 1/d^4)$,[19] which is determined by the nonradiative energy transfer from the SWNT to the metal surface. In Fig. 4(b), the calculated PL intensity enhancement using Eq. (1) is plotted as a solid line and the calculated result reproduces the maximum PL enhancement behavior at the intermediate distance. From this result, the experimentally observed PL enhancement of SWNTs on the rough Au surfaces is determined by the two competing processes of electric field enhancement, due to the surface plasmon, and the energy transfer from the SWNTs to the metal surfaces. As the electric field enhancement due to the localized surface plasmon resonance does not occur on the flat Au surface, the PL intensity is dominated by the nonradiative energy transfer process. Thus, the observed experimental result of PL quenching on the flat Au surface in Fig. 1(c) can be explained by the model described above.

In summary, we demonstrated PL intensity enhancement of single carbon nanotubes due to localized surface plasmons. The PL intensity of the SWNTs on the rough Au surface is enhanced by about three times compared to that on the fused silica surfaces. This PL enhancement arises from local field enhancement of the incident light induced by the localized surface plasmons. The improvement of the optical properties in SWNTs using the localized surface plasmon opens pathways for applying SWNTs to various optoelectronic devices and applications.

The authors thank Dr. D. Chiba and Professor T. Ono for technical support in fabricating the flat Au substrates and Shimadzu Corp. for the measurements of PL excitation spectra. This study was supported by a Grant-in-Aid for Scientific Research from the JSPS (Grant No. 20048004) and from MEXT of Japan (Grant Nos. 20340075 and 20104006).

[1] R. Saito, G. Dresselhaus, and M. S. Dresselhaus, *Physical Properties of Carbon Nanotubes* (Imperial College Press, London, 1998).
[2] P. Avouris, M. Freitag, and V. Perebeinos, Nat. Photonics **2**, 341 (2008).
[3] M.-J. O'Connell, S. M. Bachilo, C. B. Huffman, V. C. Moore, M. S. Strano, E. H. Haroz, K. L. Rialon, P. J. Boul, W. H. Noon, C. Kittrell, J. Ma, R. H. Hauge, R. B. Weisman, and R. E. Smalley, Science **297**, 593 (2002).
[4] F. Wang, G. Dukovic, L. E. Brus, and T. F. Heinz, Science **308**, 838 (2005).
[5] J. A. Misewich, R. Martel, Ph. Avouris, J. C. Tsang, S. Heinze, and J. Tersoff, Science **300**, 783 (2003).
[6] A. Högele, C. Galland, M. Winger, and A. Imamoğlu, Phys. Rev. Lett. **100**, 217401 (2008).
[7] T. K. Leeuw, R. M. Reith, R. A. Simonette, M. E. Harden, P. Cherukuri, D. A. Tsyboulski, K. M. Beckingham, and R. B. Weisman, Nano Lett. **7**, 2650 (2007).
[8] J. Crochet, M. Clemens, and T. Hertel, J. Am. Chem. Soc. **129**, 8058 (2007).
[9] L. J. Carlson, S. E. Maccagnano, M. Zheng, J. Silcox, and T. D. Krauss, Nano Lett. **7**, 3698 (2007).
[10] K. T. Shimizu, W. K. Woo, E. R. Fisher, H. J. Eisler, and M. G. Bawendi, Phys. Rev. Lett. **89**, 117401 (2002).
[11] K. Okamoto, I. Niki, A. Shvartser, Y. Narukawa, T. Mukai, and A. Scherer, Nature Mater. **3**, 601 (2004).
[12] Y. Ito, K. Matsuda, and Y. Kanemitsu, Phys. Rev. B **75**, 033309 (2007).
[13] K. Hosoki, T. Tayagaki, S. Yamamoto, K. Matsuda, and Y. Kanemitsu, Phys. Rev. Lett. **100**, 207404 (2008).
[14] A. Nish, J.-Y. Hwang, J. Doig, and R. J. Nicholas, Nat. Nanotechnol. **2**, 640 (2007).
[15] S. M. Bachilo, M. S. Strano, C. Kittrell, R. H. Hauge, R. E. Smalley, and R. B. Weisman, Science **298**, 2361 (2002).
[16] J. I. Paredes and M. Burghard, Langmuir **20**, 5149 (2004).
[17] A. O. Govorov, G. W. Bryant, W. Zhang, T. Skeini, J. Lee, N. Kotov, J. M. Slocik, and R. R. Naik, Nano Lett. **6**, 984 (2006).
[18] K. Matsuda, Y. Ito, and Y. Kanemitsu, Appl. Phys. Lett. **92**, 211911 (2008).
[19] B. N. J. Persson and N. D. Lang, Phys. Rev. B **26**, 5409 (1982).